Alternation of Melting Points in Odd- and Even-Numbered Monoacid Triacylglycerols

Arjen van Langevelde, René Peschar,* and Henk Schenk

Laboratory for Crystallography, Institute of Molecular Chemistry (IMC), Universiteit van Amsterdam, Nieuwe Achtergracht 166, 1018 WV Amsterdam, The Netherlands

Received October 5, 2000. Revised Manuscript Received December 4, 2000

Alternation of melting points in the series of odd- and even-numbered monoacid triacylglycerols has been known for a long time, but hitherto little experimental evidence has been available to support existing theories. In this paper the melting point alternation of β-$C_nC_nC_n$-type triacylglycerols is discussed, based on the crystal structures of β-$C_nC_nC_n$ (n = number of C atoms per hydrocarbon chain = 10, 12, 14, 16, 18 and n = 13, described in this paper). The crystal structure of β-1,2,3-tris(tridecanoyl)glycerol (β-$C_{13}C_{13}C_{13}$) has been determined from high-resolution synchrotron X-ray powder diffraction data and is presented here. Grid search and Rietveld refinement have been used to determine and refine the structure, respectively. Like the even-numbered monoacid triacylglycerols, β-$C_{13}C_{13}C_{13}$ is crystallized in an asymmetric tuning-fork conformation and its acyl chains are laterally packed, resulting in a layered structure. Within a molecular layer, the odd- and even-numbered monoacid triacylglycerols are identically packed, but the packing of adjacent molecular layers is different, clarifying the alternation of melting points.

Introduction

Many organic molecules, in particular those having long hydrocarbon chains, show polymorphic behavior: the hydrocarbon chains may pack in different ways, resulting in complex melt and crystallization properties. Many homologous series of long-chain organic molecules (having more than 10 C atoms/*n*-hydrocarbon chain), like *n*-alkanes, fatty acids, and triacylglycerols (TAGs), also show alternation of melting points: the melting point does not increase proportionally with the chain length, but series members with an odd number of C atoms per chain melt at a relatively lower temperature than the neighboring even-numbered members do. Because of these physical properties, long-chain molecules are intriguing research objects.

Melting point alternation has been known for a long time, but explanations put forward were difficult to verify (experimentally) at the atomic level because of a lack of crystal-structure information of long-chain organic molecules. Larsson[1] and Boese et al.[2] have reviewed these melting point alternation theories. Larsson explained melting point alternation for all types of long-chain compounds by differences in packing densities at the layer interface.[1] In his consideration, layers are regarded where only methyl groups constitute the terminal planes. The molecular arrangement within the layers of a homologous series is expected to be the same for even and odd members, but the stacking of layers may be different. Melting point alternation is expected when the structure of the terminal planes is different in even and odd members as occurs usually with tilted hydrocarbon chains. He explained the consequences of this theory for the various modes of lateral hydrocarbon chain packing in terms of end-group structure. For fatty acids the alternation of melting points was already correlated with differences in the estimated van der Waals interaction between the methyl-contact planes by Von Sydow.[3] For *n*-alkanes this melting point alternation theory was shown to be correct by the analysis of short (fewer than 9 C atoms/hydrocarbon chain) *n*-alkane crystal structures.[2] The intermolecular distances between the methyl end groups appear to be responsible for the alternation in the packing densities, whereas the lateral packing does not play any role. The even-numbered *n*-alkanes have optimal interaction at both chain ends. The odd-numbered ones possess this interaction at only one end; at the other end, the distances are longer, leading to a less dense packing and, consequently, a lower melting point.

For TAGs (Figure 1) three major phases exist, designated as α, β', and β, that show a monotropic phase behavior ($\alpha \rightarrow \beta'$, $\alpha \rightarrow \beta' \rightarrow \beta$, or $\alpha \rightarrow \beta$).[4] Melting point alternation has been observed only for the β phase. Larsson concluded that the melting points of the β' phase of TAGs do not alternate because the hydrocarbon chains are arranged according to the orthorhombic subcell[5] $O_\perp$ for which the packing density over the methyl gap will be roughly the same in even and odd members of a series of TAGs.[1] Simultaneously with the melting points, the long *d*-spacing values of the β-$C_nC_nC_n$-type (n = number of C atoms per hydrocarbon chain)

(1) Larsson, K. *J. Am. Oil Chem. Soc.* **1966**, *43*, 559.
(2) Boese, R.; Weiss, H.-C.; Bläser, D. *Angew. Chem., Int. Ed. Engl.* **1999**, *38*, 988.
(3) Von Sydow, E. *Arkiv Kemi* **1956**, *9*, 231.
(4) Hagemann, J. W. In *Crystallization and polymorphism of fats and acids*; Garti, N., Sato, K., Eds.; Marcel Dekker Inc.: New York, 1988; pp 9−96.
(5) Abrahamssson, S.; Dahlén, B.; Löfgren, H.; Pascher, I. *Prog. Chem. Fats Lipids* **1978**, *16*, 125.

10.1021/cm001190f CCC: $20.00
Published on Web 02/10/2001

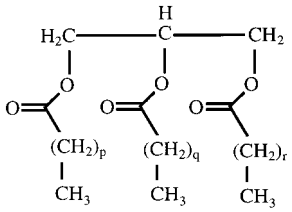

Figure 1. General chemical structure diagram of triacylglycerols. In case of monoacid triacylglycerols, $p = q = r$ is also denoted as $n + 2$. For example, $C_{13}C_{13}C_{13}$ has $p = q = r = 11$.

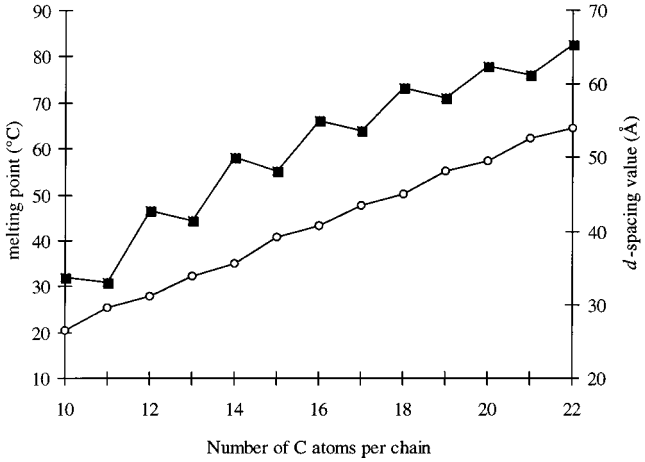

Figure 2. Melting points (black squares) and long *d*-spacing values (open circles) vs number of C atoms per chain of mono acid triacylglycerols.[6]

TAG series alternate, which may be an indication of a less dense packing for the odd-numbered series members[6] (Figure 2). Obviously, the packing density is determined by the unit-cell volume and the molecular weights.

Nowadays, crystal structures of the β-$C_nC_nC_n$-type (n = even) TAG series are known,[7] so a crystal structure of a series member with n = odd is expected to provide experimental evidence to assess the melting point alternation theories. Here we report the crystal structure of such a series member, the β phase of 1,2,3-tris-(tridecanoyl)glycerol (β-$C_{13}C_{13}C_{13}$). The structure has been determined from high-resolution synchrotron X-ray powder diffraction (XRPD) data. Because the β-$C_nC_nC_n$-type (n = even, n = 10−18) TAG series is structurally homologous, it is expected that the crystal structures of the other odd-numbered longer series members (n = odd, $n > 13$) are structurally homologous to the structure of β-$C_{13}C_{13}C_{13}$, except for a difference in chain length. On the basis of the structure β-$C_{13}C_{13}C_{13}$ and the known structures of the β-$C_nC_nC_n$-type (n = even) TAG series, an explanation of the alternation of melting points will be given.

Experimental Section

Samples, Sample Preparation, and Data Collection. $C_{13}C_{13}C_{13}$ was purchased as a colorless crystalline powder from Sigma Chemical Co. (St. Louis, MO) with a purity of approximately 99%. From a sample an XRPD photograph was made using an Enraf-Nonius FR 552 Guinier Johansson camera (Enraf-Nonius, Delft, The Netherlands) equipped with a Johansson monochromator[8] using Cu Kα_1 radiation (λ = 1.540 60 Å). The sample was prepared by pressing the powder to a thin layer onto Mylar foil. To improve particle statistics, the sample holder was rotated in the specimen plane. For indexing the pattern, the accurate positions of 50 lines were collected by reading out the Guinier photograph with an optical instrument.

An XRPD pattern of $C_{13}C_{13}C_{13}$ was also made at the high-resolution X-ray powder diffractometer stationed at BM16 (ESRF, Grenoble, France)[9] with a fixed wavelength of 0.850 05 Å. The diffractometer was equipped with a cryogenic gas cooling system for measurements at low temperatures. For data collection a capillary with a diameter of 1.5 mm was filled with powder and rotated during exposure. Continuous scans were made at T = 243 K from $2\theta = 0.0$ to 50.0° with $2\theta = 0.5°$ min^{-1} and a sampling time of 50 ms. After data collection the scans were binned at $2\theta = 0.005°$.

Structure Determination, Refinement, and Comparison. The lines obtained from the Guinier XRPD photograph of $C_{13}C_{13}C_{13}$ were indexed using the program ITO[10] and manual

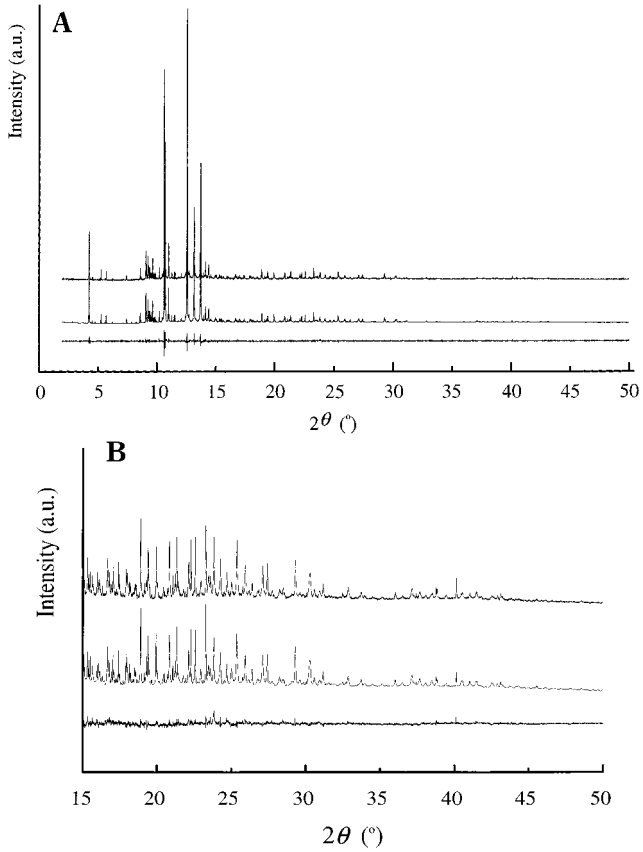

Figure 3. (A) Synchrotron powder diffraction pattern (λ = 0.850 05 Å, $2\theta = 2.0-50.0°$) of β-$C_{13}C_{13}C_{13}$ (upper), the pattern as calculated from the refined crystal structure (middle), and the difference between these patterns (lower). (B) Synchrotron powder diffraction pattern (λ = 0.850 05 Å, $2\theta = 15.0-50.0°$) of β-$C_{13}C_{13}C_{13}$ (upper), the pattern as calculated from the refined crystal structure (middle), and the difference between these patterns (lower).

(6) Lutton, E. S.; Fehl, A. J. *Lipids* **1970**, *5*, 90.

(7) (a) Gibon, V.; Blanpain, P.; Norberg, B.; Durant, F. *Bull. Soc. Chim. Belg.* **1984**, *93*, 27. (b) Jensen, L. H.; Mabis, A. J. *Acta Crystallogr.* **1966**, *21*, 770. (c) Van Langevelde, A.; Van Malssen, K.; Hollander, F.; Peschar, R.; Schenk, H. *Acta Crystallogr.* **1999**, *B55*, 114. (d) Van Langevelde, A.; Peschar, R.; Schenk, H. *Acta Crystallogr.* **2001**, *B57*, in press.

(8) Roberts, B. W.; Parrish, W. In *International Tables for Crystallography*; MacGillavry, C. H., Rieck, G. D., Eds.; Kynoch Press: Birmingham, U.K., 1962; Vol. III, pp 73−88.

(9) Fitch, A. N. In *Materials Science Forum*; Cernik, R. J., Delhez, R., Mittemeijer, E. J., Eds.; Trans Tech Publications: Aedermannsdorf, Switzerland, 1996; Vol. 228, pp 219−222.

(10) Visser, J. W. *J. Appl. Crystallogr.* **1969**, *2*, 89.

Table 1. Unit Cell Parameters for β-$C_{13}C_{13}C_{13}$ at $T = 243$ K

cell param	refined	transformed	transformed[a,b]	transformed	transformed[a]
a (Å)	11.9438(6)	11.94	11.94	11.94	11.94
b (Å)	38.568(1)	41.34	41.34	36.48	36.48
c (Å)	5.4484(3)	5.45	5.45	5.45	5.45
α (deg)	75.117(4)	108.1	71.9	107.1	72.9
β (deg)	100.291(5)	100.3	100.3	100.3	100.3
γ (deg)	116.073(7)	58.2	121.8	74.3	105.7
transformation matrix		$\begin{matrix}1&0&0\\3&1&\bar{3}\\0&0&1\end{matrix}$	$\begin{matrix}\bar{1}&0&0\\\bar{3}&\bar{1}&3\\0&0&1\end{matrix}$	$\begin{matrix}1&0&0\\2&1&\bar{3}\\0&0&1\end{matrix}$	$\begin{matrix}\bar{1}&0&0\\\bar{2}&\bar{1}&3\\0&0&1\end{matrix}$

[a] Coordinate system inverts upon transformation. [b] Unit cell setting used for crystal-structure comparison.

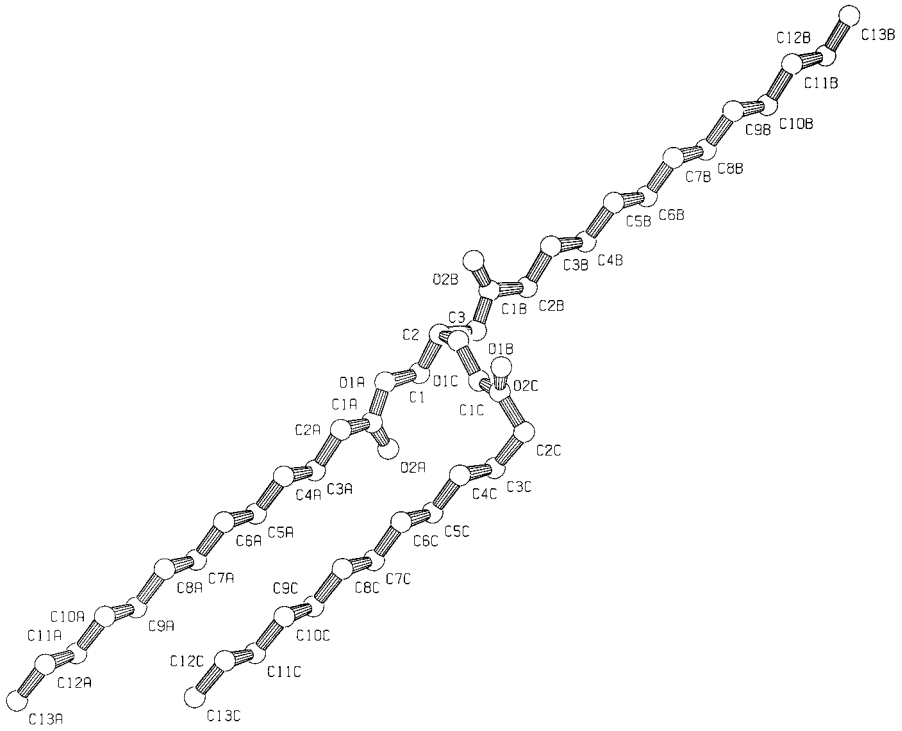

Figure 4. PLATON[19] representation of the crystal structure of β-$C_{13}C_{13}C_{13}$.

interference. The resulting unit cell parameters were refined on the synchrotron data using the program UnitCell.[11] Accurate reflection intensities have been obtained using a full-pattern decomposition (FPD) procedure: the high-resolution synchrotron XRPD pattern was fitted by employing a split-type pseudo-Voigt peak-profile function[12] and decomposed using the program MRIA.[13] A starting model for β-$C_{13}C_{13}C_{13}$ was made from the crystal structure of β-1,2,3-tris(hexadecanoyl)glycerol (β-$C_{16}C_{16}C_{16}$ or β-PPP)[7c] by replacing the terminating $-CH_2CH_2CH_3$ moieties of the palmitic chains with H atoms using the program Cerius^2.[14] To locate this possible model in the asymmetric unit, a grid-search procedure[13] was applied to 300 low-order reflections obtained by the FPD procedure. The obtained translational and rotational parameters were refined, followed by a full-pattern Rietveld refinement (RR). Soft restraints were applied to the atomic distances (σ is ~1% of the ideal bond lengths) during RR. Under these conditions the coordinates of all atoms (O, C, and H) as well as isotropic atomic displacement parameters (U_{iso}) were refined. The U_{iso} values of all C atoms as well as the U_{iso} values for all O atoms were coupled; the U_{iso} values for H atoms were fixed at 0.05 Å^2. The preferred orientation was refined using the first 14 coefficients of the symmetrized harmonics-expansion method.[16]

To figure out the differences in crystal packing which may explain the melting point alternation in the β-$C_nC_nC_n$-type TAG series, the crystal structure of β-$C_{13}C_{13}C_{13}$ has been compared with the known crystal structures of the even-numbered β-$C_nC_nC_n$-type ($n = 10-18$) TAGs. The structures were matched by minimizing the distance between corresponding C and O atoms, resulting in an overall root-mean-square (rms) value expressing the quality of the fit. Matched crystal structures were visually analyzed using the program PLUVA v3.0.[17] Distances between chain-terminating C atoms of two adjacent chain layers were calculated for the known structures of the $C_nC_nC_n$-type TAG series using the program BONDLA.[18] Occupiable volumes (unit cell volume not occupied by atoms but large enough to fit in atomic probes with a certain radius) were calculated using the program Cerius^2 [14] employing a probe with 1.6 Å radius and atomic van der Waals radii.

(11) Holland, T. J. B.; Redfern, S. A. T. *Miner. Magn.* **1997**, *61*, 65.
(12) Toraya, H. *J. Appl. Crystallogr.* **1986**, *19*, 440.
(13) Zlokazov, V. B.; Chernyshev, V. V. *J. Appl. Crystallogr.* **1992**, *25*, 447.
(14) Cerius^2, Release 2.0, Biosym/Molecular Simulations Inc., San Diego.
(15) Chernyshev, V. V.; Schenk, H. *Z. Kristallogr.* **1998**, *213*, 1.
(16) (a) Ahtee, M.; Nurmela, M.; Suortti, P.; Järvinen, M. *J. Appl. Crystallogr.* **1989**, *22*, 261. (b) Järvinen, M. *J. Appl. Crystallogr.* **1993**, *26*, 525.
(17) Driessen, R. A. J.; Loopstra, B. O.; De Bruijn, D. P.; Kuipers, H. P. C. E.; Schenk, H. *J. Comput.-Aided Mol. Des.* **1988**, *2*, 225.
(18) Hall, S. R.; King, G. S. D.; Stewart, J. M. Xtal, Version 3.5; Universities of Western Australia, Australia, Geneva, Switzerland, and Maryland.
(19) Spek, A. L. PLATON, a multipurpose crystallographic tool; Utrecht University, Utrecht, The Netherlands.

Table 2. Fractional Atomic Coordinates of β-$C_{13}C_{13}C_{13}$ at $T = 243$ K after Rietveld Refinement[a]

atom	*X*	*Y*	*Z*
C1	0.071	0.479	−0.174
C2	0.191	0.508	−0.068
C3	0.280	0.490	0.057
O1a	0.015	0.449	0.049
C1a	−0.066	0.413	0.005
O2a	−0.088	0.406	−0.206
C2a	−0.107	0.383	0.242
C3a	−0.230	0.347	0.193
C4a	−0.268	0.317	0.442
C5a	−0.392	0.283	0.404
C6a	−0.434	0.252	0.648
C7a	−0.561	0.218	0.603
C8a	−0.603	0.187	0.839
C9a	−0.732	0.153	0.794
C10a	−0.773	0.121	1.034
C11a	−0.904	0.089	0.982
C12a	−0.948	0.055	1.217
C13a	−1.080	0.024	1.157
O1b	0.248	0.534	−0.298
C1b	0.328	0.570	−0.261
O2b	0.349	0.582	−0.063
C2b	0.383	0.597	−0.512
C3b	0.502	0.633	−0.460
C4b	0.547	0.662	−0.714
C5b	0.675	0.697	−0.670
C6b	0.718	0.727	−0.921
C7b	0.841	0.761	−0.877
C8b	0.883	0.792	−1.119
C9b	1.010	0.826	−1.072
C10b	1.057	0.856	−1.317
C11b	1.177	0.892	−1.268
C12b	1.225	0.923	−1.511
C13b	1.342	0.959	−1.461
O1c	0.283	0.463	−0.086
C1c	0.359	0.447	−0.026
O2c	0.433	0.453	0.169
C2c	0.365	0.423	−0.197
C3c	0.227	0.393	−0.267
C4c	0.178	0.362	−0.019
C5c	0.050	0.329	−0.073
C6c	0.009	0.297	0.170
C7c	−0.117	0.263	0.123
C8c	−0.158	0.232	0.366
C9c	−0.288	0.198	0.323
C10c	−0.323	0.165	0.564
C11c	−0.453	0.132	0.520
C12c	−0.487	0.101	0.772
C13c	−0.617	0.067	0.738

[a] Cell parameters of β-$C_{13}C_{13}C_{13}$: $a = 11.9438(6)$, $b = 38.568(1)$, and $c = 5.4484(3)$ Å; $\alpha = 75.117(4)$, $\beta = 100.291(5)$, and $\gamma = 116.073(3)°$. The volume is 2172.5(1) Å^3, and the space group is $P\bar{1}$; with $Z = 2$ the calculated density is 1.04 g cm^{-3}. U_{iso} (Å^2) values are 0.033 and 0.023 for C and O atoms, respectively.

Table 3. Selected Geometric Parameters (Å^2 and deg) for β-$C_{13}C_{13}C_{13}$

C1−O1a	1.47	C4b−C5b	1.56
C1−C2	1.51	C5b−C6b	1.55
C2−O1b	1.45	C6b−C7b	1.51
C2−C3	1.49	C7b−C8b	1.53
C3−O1c	1.45	C8b−C9b	1.54
O1a−C1a	1.35	C9b−C10b	1.52
C1a−O2a	1.20	C10b−C11b	1.54
C1a−C2a	1.48	C11b−C12b	1.55
C2a−C3a	1.56	C12b−C13b	1.50
C3a−C4a	1.52	O1c−C1c	1.28
C4a−C5a	1.52	C1c−O2c	1.26
C5a−C6a	1.54	C1c−C2c	1.51
C6a−C7a	1.53	C2c−C3c	1.59
C7a−C8a	1.52	C3c−C4c	1.52
C8a−C9a	1.55	C4c−C5c	1.53
C9a−C10a	1.52	C5c−C6c	1.55
C10a−C11a	1.55	C6c−C7c	1.53
C11a−C12a	1.54	C7c−C8c	1.53
C12a−C13a	1.55	C8c−C9c	1.55
O1b−C1b	1.35	C9c−C10c	1.55
C1b−O2b	1.21	C10c−C11c	1.53
C1b−C2b	1.54	C11c−C12c	1.56
C2b−C3b	1.53	C12c−C13c	1.54
C3b−C4b	1.54		
O1a−C1−C2	105	C2b−C3b−C4b	110
O1b−C2−C1	102	C5b−C4b−C3b	111
O1b−C2−C3	104	C4b−C5b−C6b	111
C1−C2−C3	113	C7b−C6b−C5b	111
O1c−C3−C2	112	C8b−C7b−C6b	112
C1a−O1a−C1	117	C7b−C8b−C9b	112
O2a−C1a−O1a	121	C8b−C9b−C10b	112
O2a−C1a−C2a	125	C9b−C10b−C11b	112
O1a−C1a−C2a	113	C12b−C11b−C10b	114
C1a−C2a−C3a	112	C11b−C12b−C13b	113
C4a−C3a−C2a	110	C1c−O1c−C3	123
C5a−C4a−C3a	111	O2c−C1c−O1c	118
C4a−C5a−C6a	114	O2c−C1c−C2c	121
C7a−C6a−C5a	112	O1c−C1c−C2c	120
C8a−C7a−−C6a	113	C3c−C2c−C1c	109
C7a−C8a−C9a	113	C4c−C3c−C2c	107
C10a−C9a−C8a	113	C3c−C4c−C5c	111
C11a−C10a−C9a	110	C6c−C5c−C4c	110
C10a−C11a−C12a	112	C5c−C6c−C7c	112
C13a−C12a−C11a	110	C8c−C7c−C6c	112
C1b−O1b−C2	112	C7c−C8c−C9c	112
O2b−C1b−O1b	126	C10c−C9c−C8c	111
O2b−C1b−C2b	124	C9c−C10c−C11c	111
O1b−C1b−C2b	111	C12c−C11c−C10c	109
C1b−C2b−C3b	111	C11c−C12c−C13c	111

Results and Discussion

The chemical structure diagram of β-$C_{13}C_{13}C_{13}$ is shown in Figure 1. The unit cell parameters of β-$C_{13}C_{13}C_{13}$ (Table 1) were refined on the synchrotron XRPD pattern using the 2θ range of 2.0−28.0°. The space group is $P\bar{1}$ and with one $C_{42}H_{80}O_6$ molecule per asymmetric unit the calculated density is 1.04 g cm^{-3}. The FPD procedure was applied to the 2.0−28.0° 2θ part of the synchrotron XRPD pattern and resulted in an R_p value of 8.7%, an R_{wp} of 13.6%, and a χ^2 of 13.6. The RR procedure was applied to a 2θ range of 2.0−50.0°, resulting in a final fit between the calculated and experimental XRPD pattern with an R_p value of 4.7%, an R_{wp} of 5.3%, an R_{Bragg} of 10.1%, and an χ^2 of 2.0 (Figure 3). Without correction for the preferred orientation, the R_p value was 6.1%, the R_{wp} value 6.8%, the R_{Bragg} value 13.2%, and the χ^2 value 2.6. The refined crystal structure of β-$C_{13}C_{13}C_{13}$ is shown in Figure 4, and the fractional atomic coordinates and selected geometric parameters are listed in Tables 2 and 3, respectively.

To compare the crystal structure of β-$C_{13}C_{13}C_{13}$ with the structure of the even-numbered $C_nC_nC_n$-type TAG series, its unit cell was transformed to make the longest unit cell axis parallel to the hydrocarbon chains. However, no crystallographic-legitimated transformation matrix has been found which transforms the longest unit cell axis parallel to the chains. Therefore, one of the two unit cell settings with the *b* axis most parallel to the acyl chains has been chosen to be used in the further considerations (Table 1).

Like the even-numbered series members, β-$C_{13}C_{13}C_{13}$ was crystallized in an asymmetric tuning-fork conformation (Figure 4). The zigzag planes of the acyl chains are parallel packed, which is common to the crystal packing of the β phase, forming layers of laterally packed acyl chains bordered by either a methyl end group plane or glycerol moieties. The conformations of

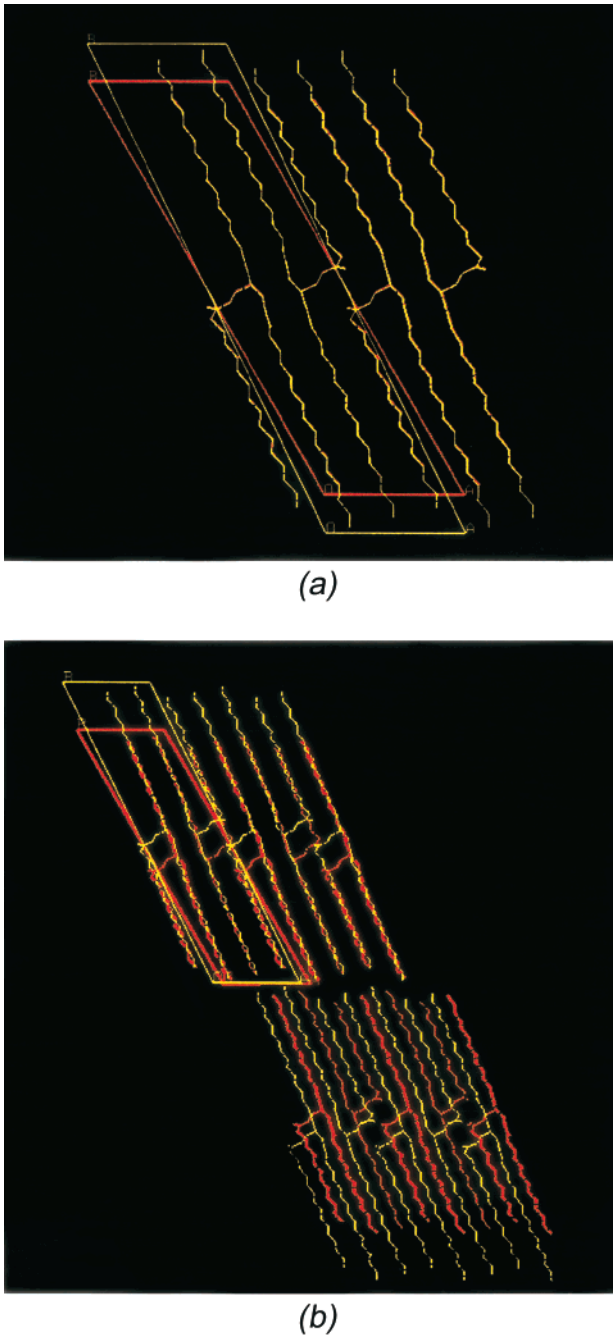

Figure 5. Crystal packing of β-$C_{13}C_{13}C_{13}$ (red) and β-PPP (green with the overlap in yellow) with the *c* axis perpendicular to the plane of the paper showing the (a) identical crystal packing of odd- and even-numbered series members within one molecular layer and (b) the different positions of two adjacent molecular layers.

the β-$C_{13}C_{13}C_{13}$ molecules and the even-numbered one are almost identical, besides the difference in chain length, as expressed by the low overall rms value of 0.036, obtained by matching β-$C_{13}C_{13}C_{13}$ and β-PPP.[7c] Also the packing of the β-$C_{13}C_{13}C_{13}$ molecules within one layer of molecules, constituting two chain layers linked by glycerol moieties, is almost identical to that of the even-numbered series (Figure 5a).

Although the lateral chain packing and the associated subcell of even- and odd-numbered series members are identical, the observed high-intensity *d*-spacing values and corresponding reflections in the characteristic region of their X-ray powder diffraction patterns (*d*-spacing values between 3 and 6 Å) are not the same (Table 4), because the subcell of β-$C_{13}C_{13}C_{13}$ is oriented somewhat differently in the unit cell as compared to the even-numbered series members. Therefore, the high-intensity reflections originating from the lateral chain packing of β-$C_{13}C_{13}C_{13}$ differ from the even-numbered ones in both the indices (especially the *k* index) and *d*-spacing values.

Table 4. Characteristic *d*-Spacing Values (Å) for β-TAGs[a]

β-$C_{13}C_{13}C_{13}$		β-PPP[7c]	
hkl	*d*(*hkl*)	*hkl*	*d*(*hkl*)
0 0 1	5.18	0 0 1	5.23
1 $\bar{0}$ 1	4.58	1 0 1	4.58
1 $\bar{1}$ 1	4.54	1 $\bar{1}$ 1	4.55
2 $\bar{1}$ $\bar{1}$	3.87	2 0 $\bar{1}$	3.82
3 $\bar{2}$ 0	3.69	3 $\bar{1}$ 0	3.64
3 $\bar{1}$ 0	3.55		

[a] Cell parameters of β-$C_{13}C_{13}C_{13}$: $a = 11.94$, $b = 41.34$, and $c = 5.45$ Å; $\alpha = 71.9$, $\beta = 100.3$, and $\gamma = 121.8°$. Cell parameters of β-PPP: $a = 11.95$, $b = 46.84$, and $c = 5.45$ Å; $\alpha = 73.8$, $\beta = 100.2$, and $\gamma = 118.1°$.

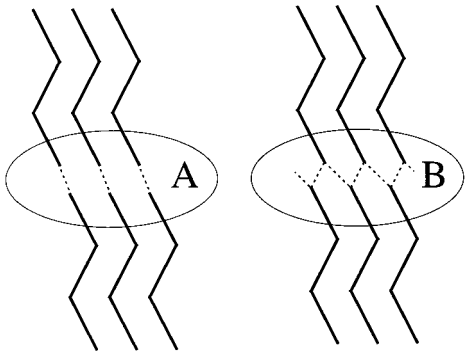

Figure 6. Schematic representation of (a) an in-line and (b) a zigzag methyl end group interaction.

Unlike the crystal packing within one molecular layer, the mutual position of two adjacent layers of β-$C_{13}C_{13}C_{13}$ molecules differs from that in the even-numbered series members. Matching the hydrocarbon chains of β-$C_{13}C_{13}C_{13}$ and β-PPP with the terminating C atoms in one plane revealed that the symmetry-equivalent β-$C_{13}C_{13}C_{13}$ molecules of the adjacent layer are positioned 2 Å further away in both the *a* and *c* directions in comparison to two successive β-PPP molecular layers (Figure 5b). As a result, the hydrocarbon chain ends are positioned in an in-line manner (Figure 6a) like the even-numbered ones rather than in a zigzag way (Figure 6b). However, the methyl end group interaction of β-$C_{13}C_{13}C_{13}$ is not identical to the methyl end group interaction of the even-numbered ones, which is shown by the distances between the terminating C atoms of adjacent molecular layers (Table 5). The C13a···C13c and C13b···C13b distances of β-$C_{13}C_{13}C_{13}$ are larger than the corresponding distances of the even-numbered series members. Furthermore, between two adjacent molecular layers of β-$C_{13}C_{13}C_{13}$ exists a larger occupiable volume than that for the even-numbered series members, as can be concluded from the significantly larger percentage of occupiable volume per unit cell for β-$C_{13}C_{13}C_{13}$ (Table 6). Apparently, this in-line configuration is still energetically favorable over the zigzag option.

On the basis of the observed differences between the crystal structure of β-$C_{13}C_{13}C_{13}$ and the even-numbered

Table 5. Shortest Distances (<4.4 Å) between Methyl End Atoms of Adjacent Chain Layers for β-TAGs[a]

	atom number *x*	C*x*a···C*x*c (Å)		C*x*b···C*x*b (Å)		C*x*a···C*x*a (Å)
CCC[7a]	10	3.73	4.09	3.66	4.01	4.32
LLL[7b]	12	3.70	4.08	3.65	3.98	4.32
$C_{13}C_{13}C_{13}$	13	3.79	>4.4	3.73	>4.4	3.99
MMM[7d]	14	3.55	4.05	3.54	3.81	4.23
PPP[7c]	16	3.67	4.01	3.65	3.94	4.28
SSS[7d]	18	3.65	4.02	3.66	4.05	4.35

[a] CCC = 1,2,3-tris(decanoyl)glycerol; LLL = 1,2,3-tris(dodecanoyl)glycerol; $C_{13}C_{13}C_{13}$ = 1,2,3-tris(tridecanoyl)glycerol; MMM = 1,2,3-tris(tetradecanoyl)glycerol; PPP = 1,2,3-tris(hexadecanoyl)-glycerol; SSS = 1,2,3-tris(octadecanoyl)glycerol.

Table 6. Occupiable Volume per Unit Cell for β-TAGs[a]

	unit cell volume (Å^3)	occupiable volume (Å^3/unit cell)	% occupiable volume per unit cell volume
CCC[7b]	1762(8)	55.5	3.15
LLL[7a]	2030(5)	65.3	3.22
$C_{13}C_{13}C_{13}$	2172.5(1)	72.3	3.33
MMM[7d]	2314.7(2)	76.5	3.30
PPP[7c]	2581.1(5)	86.8	3.36
SSS[7d]	2879.6(2)	98.7	3.43

[a] CCC = 1,2,3-tris(decanoyl)glycerol; LLL = 1,2,3-tris(dodecanoyl)glycerol; $C_{13}C_{13}C_{13}$ = 1,2,3-tris(tridecanoyl)glycerol; MMM = 1,2,3-tris(tetradecanoyl)glycerol; PPP = 1,2,3-tris(hexadecanoyl)-glycerol; SSS = 1,2,3-tris(octadecanoyl)glycerol.

series members, the alternation of melting points between odd- and even-numbered series members can be understood. The energy necessary to melt crystalline material is negatively related to the lattice energy. The lattice energy of these $C_nC_nC_n$-type crystal structures can be considered to consist of two parts: (i) the lattice energy of the crystal packing within a molecular layer and (ii) the lattice energy between two adjacent molecular layers. The first part increases linearly with lengthening of the hydrocarbon chains, while the second part remains constant, resulting in an expected linear increase of the melting point with increasing chain length. However, because the interaction between two adjacent molecular layers of even-numbered series members is stronger than that for the odd-numbered ones, the melting points of odd- and even-numbered series members alternate. With increasing chain length, the ratio between the two lattice energy parts increases in the end. So, the difference between the melting points of odd- and even-numbered series members decreases with increasing chain length (Figure 2).

The above analysis implies, admittedly still based on one odd-membered $C_nC_nC_n$ crystal structure, that the alternation of melting points for TAGs indeed originates from different interactions at the methyl end group region for odd- and even-numbered series members.[1] Nevertheless, the interaction at the methyl ends of odd-numbered TAGs is comparable to the interaction observed for odd-numbered *n*-alkanes.[2] These latter molecules also preferably obtain a more in-line methyl end group interaction (Figure 6), resulting in a less dense packing in this methyl end group region. Soon additional experimental evidence is expected to be provided by the analysis of the structures of β-$C_{15}C_{15}C_{15}$, β-$C_{17}C_{17}C_{17}$, and β-$C_{19}C_{19}C_{19}$ that is currently in progress.

Acknowledgment. The investigations are supported by The Netherlands Foundation for Chemical Research (NWO/CW) with financial aid from The Netherlands Technology Foundation (STW). The authors thank the ESRF (Grenoble, France) for the opportunity to perform the synchrotron diffraction experiments and Dr. A. Fitch and Dr. E. Doryhee for their invaluable help at beamline BM16. They also thank E. J. Sonneveld for making the Guinier X-ray powder diffractogram and Dr. K. Goubitz for performing geometry calculations.

CM001190F